Toxicity and Carcinogenicity Mechanisms of Fibrous Antigorite

Venera Cardile[1*], Laura Lombardo[1], Elena Belluso[2], Annamaria Panico[3], Silvana Capella[2], and Michael Balazy[4*]

[1]Department of Physiological Sciences, University of Catania, Italy
[2]Department of Mineralogical and Petrological Sciences, University of Turin, Turin, CNR IGG-Sezione I Torino, Italy
[3]Department of Pharmaceutical Sciences, University of Catania, Catania, Italy
[4]Department of Pharmacology, New York Medical College, Valhalla, NY, USA
[*]Correspondence to Dr. Venera Cardile. E-mail: cardile@unict.it or Dr. Michael Balazy. Email: michael_balazy@nymc.edu

---

Abstract: We studied the effects of fibrous antigorite on mesothelial MeT-5A and monocyte-macrophage J774 cell lines to further understand cellular mechanisms induced by asbestos fibers leading to lung damage and cancer. Antigorite is a mineral with asbestiform properties, which tends to associate with chrysotile or tremolite, and frequently occurs as the predominant mineral in the veins of several serpentinite rocks found abundantly in the Western Alps. Particles containing antigorite are more abundant in the breathing air of this region than those typically found in urban ambient air. Exposure of MeT-5A and J774 cells to fibrous antigorite at concentrations of 5-100 µg/ml for 72 hr induced dose-dependent cytotoxicity. Antigorite also stimulated the ROS production, induced the generation of nitrite and PGE_2. MeT-5A cells were more sensitive to antigorite than J774 cells. The results of this study revealed that the fibrous antigorite stimulates cyclooxygenase and formation of hydroxyl and nitric oxide radicals. These changes represent early cellular responses to antigorite fibers, which lead to a host of pathological and neoplastic conditions because free radicals and PGE_2 play important roles as mediators of tumor pathogenesis. Understanding the mechanisms of the cellular responses to antigorite and other asbestos particles should be helpful in designing rational prevention and treatment approaches.

Keywords: Antigorite; asbestos fibers; free radicals; inflammation; lung cancer; oxidative stress; toxicity, cyclooxygenase.

List of Abbreviations

COX	Cyclooxygenase
DCFH-DA	2'7'-dichlorodihydrofluorescein diacetate
DMSO	Dimethylsulphoxide
ELISA	Enzyme-linked immunosorbent assay
LDH	Lactate dehydrogenase
MTT	3-(4,5-dimethylthiazol-2-yl)-2,5-diphenyl test
NF-$\kappa\beta$	Nuclear factor kappa B
$NO^{\bullet}$	Nitric oxide
PBS	Phosphate saline buffer
PGE_2	Prostaglandin E_2
RNS	Reactive nitrogen species
ROS	Reactive oxygen species
SEM-EDS	Scanning electron microscopy-energy dispersive spectrometry
TEM-EDS	Transmission electronic microscopy-energy dispersive spectrometry
XRPD	X-ray powder diffractometry

Introduction

Exposure to asbestos in industrial settings and in the area of collapsed buldings has been linked to the development of lung and pleural diseases including lung cancer, asbestosis and mesothelioma [1, 2]. Asbestos is a family of six distinct silicate fibres sub-grouped as serpentine (chrysotile) and amphibole (amosite,

crocidolite, anthophyllite, tremolite and actinolite) each having unique chemistry and morphology. Extensive studies performed *in vivo* and *in vitro* have identified several pathogenic mechanisms of asbestos-related diseases; however, asbestos-dependent carcinogenic and mutagenic mechanisms are still incompletely understood [3]. Over the last few years, the awareness of possible health hazards related to environmental exposure to natural asbestos has been increasing. Natural rock aging and the use of crushed serpentinite for paving roads and other surfaces contribute to increased levels of asbestos fibers in the air in some parts of the world. Air samples taken in the vicinity of serpentine-paved roads show that chrysotile concentrations are about 10^3 times greater than those typically found in urban ambient air [4].

Recently, the asbestiform minerals filling the veins of serpentinite rocks outcropping in the Western Alps (Piemonte, Italy) have been systematically studied by using optical, X-ray, SEM-EDS and TEM-EDS techniques. In addition to chrysotile, tremolite, and actinolite asbestos, the following minerals with asbestiform morphology have been found: balangeroite, carlosturanite, antigorite, diopside, olivine, brugnatellite and brucite [5-7]. At least two species of these mineral fibres are present in all serpentinite rocks. For example, in the chrysotile from Balangero mine, closed in 1990, the asbestos was associated with fibers of balangeroite and diopside. The toxic effects of some of these airborne mineral fibres, (i.e. chrysotile) have been well established, whereas fibrous antigorite, although very abundant in serpentinite rocks of the Western Alps, has been much less characterized. Antigorite is a silicate mineral, very similar in chemical composition to chrysotile but its crystallography is much different. Its structure allows formation of massive or fibrous crystals, depending on the origin and growth conditions (Figure 1).

Figure 1: A photograph of the fibrous antigorite shown as perpendicular to vein selvages in serpentinitic rock. A 15 cm pen was used as a size reference.

The fibres of antigorite are subcentrimetric in length and ubiquitous in the serpentinites analyzed by us. These fibers are usually white, but some are light green or red because of iron salts, which may additionally play a role in their toxicity. The serpentinites from the inner Piemonte area have been suspected to pose a potential health hazard [8, 9]. Previous studies revealed that asbestos fibers containing iron induce generation of reactive oxygen (ROS) or nitrogen (RNS) species, which provoke inflammatory cytotoxic effects in cells [10, 11]. Only a small fraction of fibers shows high cytotoxicity, and certain types of fibres originating from natural sources can cause a wide variety of respiratory diseases ranging from inflammation and fibrosis to highly malignant forms of cancers.

This study aimed to examine the cellular responses of fibrous antigorite and to characterize biochemical changes induced by asbestos fibers that may lead to pulmonary damage. The effects of antigorite were studied in two cell lines: MeT-5A, a non-malignant transformed mesothelial cell line, widely known as a model of normal human mesothelial cells in studies on pleural pathology [12], and in a J774 cell line, the mouse monocyte-macrophage cell line, that allowed evaluation of cytotoxicity in alveolar macrophages as in a previous study of various silica dusts [13]. The cellular toxicity of antigorite was determined by measurement of cell viability and membrane integrity using the MTT test and LDH activity. The generation of ROS and RNS represents one of the main response mechanisms to chemical and physical stimulation and phagocytosis [14, 15]. Studies on animal models and cell cultures have indicated that fibres stimulate ROS and RNS generation and cause oxidation and/or nitrosylation of proteins, lipids and DNA [1,16]. Thus, the possible induction of oxidative stress by antigorite was examined both by performing a fluorescent analysis of intracellular ROS production, and evaluating the amount of nitrite in cell culture media.

Numerous investigations have established the cellular importance of the cyclooxygenase isoenzymes (COX-1 and COX-2), which catalyse stereospecific oxidation of arachidonic acid to prostaglandins (PGs) [17]. COX-1 is expressed constitutively in a variety of tissues and products of this enzyme are important for homeostatic processes. COX-2 is an inducible isoform activated by cytokines and growth factors that produce predominately pro-inflammatory PGs. Moreover, expression of COX-2 is upregulated in a variety of malignancies. PGE_2 has been implicated as having an important role in the pathogenesis of solid tumours through inhibition of apoptosis, facilitation of tumour cell invasiveness and stimulation of angiogenesis [17]. In the current study, we used ELISA method to reveal the role of PGE_2 in the effects of antigorite. The data obtained with antigorite were compared with those obtained with crocidolite, which due to its high toxicity has been one of the most studied asbestos amphiboles. Carbonyl iron spheres were used as a control particulate.

Materials and Methods

Cell Cultures

MeT-5A mesothelial cells (kindly provided by Prof. G. Biagini, Istituto di Morfologia Umana Normale-

Istologia, Università Politecnica delle Marche) were grown in RPMI medium (Sigma, Milan, Italy) supplemented with 10% fetal bovine serum (FBS), 1% non-essential amino acids, 2.0 mM L-glutamine, and a mixture of standard antibiotics and incubated at 37°C and 5% CO_2. The cells were routinely split (1:2) each week and used between the 4th and 5th passages. Cells from confluent cultures were detached using 0.25% trypsin in 1 mM EDTA solution and seeded in complete RPMI medium.

A mouse monocyte-macrophage tumour J774 cell line was obtained from American Type Culture Collection (Rockville, MD, USA). The cells were cultured in Dulbecco's modified Eagle's medium (DMEM) containing 10% FBS, 4.5 g/L glucose, 1 mM sodium pyruvate, 2.0 mM L-glutamine, and antibiotics (Invitrogen, Paisley, UK) and incubated at 37°C and 5% CO_2. The medium was changed every three days and subcultures were performed every 10-12 days.

Before the experiments, the cells were trypsinized, counted in a haemocytometer, plated onto 96- or 6-well plates (Costar, Cambridge, MA), and grown in a humidified 5% CO_2 incubator at 37°C.

Antigorite Isolation and Analysis

The samples of antigorite fibres were isolated from serpentinite rock collected at Blue Lake near St. Jacques in Aosta (Italy). Inspection of the sample under the stereoscopic microscope revealed the subcentrimetric grey fibres of lamellar morphology and without detectable impurities (Figure 1).

The fibres were further characterized by an X-ray Powder Diffractometer (XRPD Siemens D5000, CuKa radiation using EVA software program to determine mineral phases and comparison with PDF2 reference patterns) and a Scanning Electron Microscope equipped with an Energy Dispersive Spectrometer (SEM Cambridge Stereoscan 360; EDS Oxford INCA 200 Microanalysis suite, Pentafet detector) (Figure 2).
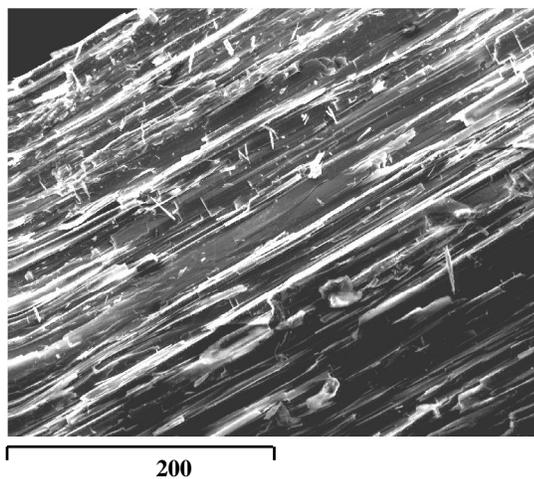

Figure 2: Secondary electron SEM image of antigorite fibre bundle.

The unequivocal identification of the fibres was obtained by analysis with a Transmission Electron Microscope (TEM Philips CM12, 120 kV, LaB6 filament) and annexed EDS (EDAX Si-Li detector PV 9800) by combined Selected Area Electron Diffraction (SAED), transmission electron imaging and analytical electron microprobe (AEM).

The X-ray diffractometry, electron crystallography and chemical characteristics were consistent with fibrous antigorite [18, 19]. The XRPD pattern showed the presence of antigorite as the predominant fiber (Figure 3).
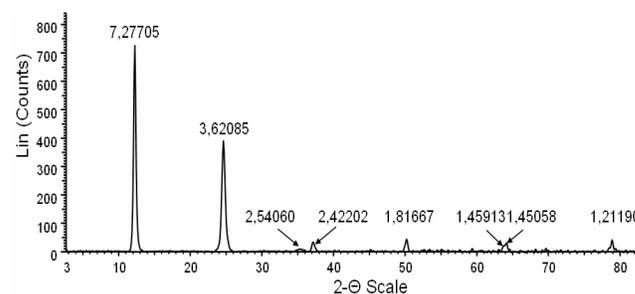

Figure3: X-ray diffraction pattern of fibrous antigorite. The interplanar reticular values (d_{hkl}) are indicated above the peaks. All d_{hkl} values and their intensities are consitent with the structure of antigorite.

This figure shows a profile of the X-ray powder diffraction (XRPD) obtained from powdered antigorite fibres. The peaks with normalized intensity greater than 5% have been used for mineral identification. The interplanar reticular values (d_{hkl}) are indicated above the corresponding peaks. All d_{hkl} values and their intensities were consitent with the structure of antigorite. The absence of peaks unrelated to this mineral indicate the sample purity (within the detection limit of the instrument, i.e. about 1%). The clean and symmetric shape of the peaks denotes high crystallinity of the fibres.

TEM investigations showed fibers being 14 to 20 µm long and 0.08 to 0.4 µm wide (Figure 4a) and of high crystallinity (Figure 4b). The chemical formula obtained from several AEM analyses was: $(Mg_{11.05}Fe_{0.53}Al_{0.21})_{12.00}(Si_{7.98}Al_{0.02})_{8.00}O_{20}(OH)_{16}$.

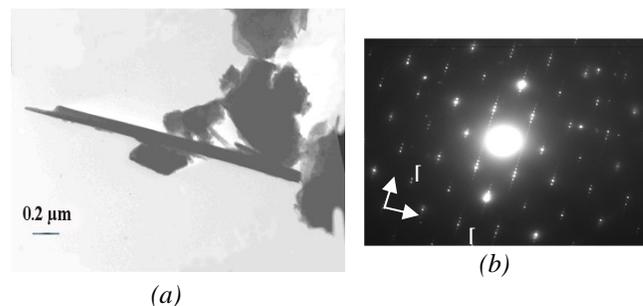*(a)*   *(b)*

Figure 4: (a) Transmission electron image of antigorite fibrils as seen perpendicularly to fibre axis, i.e. [001] crystallographic direction. (b) Selected area electron diffraction from a sample shown in (a) taken along the same crystallographic direction.

Treatments of Cells

Antigorite was weighed, suspended in culture medium by vortexing and added to the experimental cultures at concentrations of 5, 50, and 100 µg/ml containing 1923, 19231, 38461× 10^3 fibers, respectively for 72 hr before cell harvesting. Crocidolite fibres having an average length of 3.2 ± 1.0 µm and an average diameter of 0.22 ± 0.01 µm were prepared as antigorite and used as a standard reference (International Union Against Cancer). Carbonyl iron spheres (size range 1-10 µm; average particle size 4.5-5.2 µm) purchased from Sigma (Italy) were used as a control particulate at concentration of 10 µg/ml.

MTT Assay

The MTT (3-(4,5-dimethylthiazol-2-yl)-2,5-diphenyl tetrazolium bromide) proliferation assay is based on conversion by mitochondrial dehydrogenases of the substrate containing a tetrazolium ring into blue formazan, detectable spectrophotometrically [20]. The level of blue formazan is then used as indirect index of cell density. Briefly, the cell cultures were set up in flat-bottomed 200 µl microplates, incubated at 37°C in a humidified 5% CO_2/95% air mixture and treated with 5, 50 and 100 µg/ml of fibrous antigorite for 72 hr. Four hours before the end of the culture, 20 µl of 0.5% MTT in phosphate saline buffer (PBS) was added to each microwell. After the incubation with the reagent, the supernatant was removed and replaced with 100 µl of dimethylsulphoxide (DMSO). The optical density of each sample was measured with a microplate spectrophotometer reader (Titertek Multiskan, DAS, Italy) at $\lambda = 550$ nm. For each sample three measurements were performed.

LDH Release

The untreated control and antigorite treated cells were harvested, washed in PBS, mixed with lysis buffer (TrisHCl 50 mM, 20 mM EDTA, pH 7.4, 0.5% SDS), sonicated and then centrifuged at 10,000×g for 15 min. The supernatant was collected and the protein content was measured by the Bradford procedure [21]. The LDH enzymatic activity was measured by incubation of cell supernant (33 µl) of in PBS buffer (48 mM) containing pyruvate (1 mM) and 0.2 mM reduced pyridinic coenzyme (pH 7.5, final volume 1 ml). The activity of LDH was measured spectrophotometrically in culture medium and in the cellular lysates at $\lambda_{max} = 340$ nm by analysis of the NADH reduction during the pyruvate-lactate transformation [22]. The release of LDH was calculated as a percentage of the total amount, considered as the sum of the enzymatic activity present in the cellular lysate and that of the culture medium.

Reactive Oxygen Species (ROS) Analysis

Reactive species formation was estimated by using DCFH-DA as a fluorescent probe (Molecular Probes,

Eugene, OR). DCFH-DA diffuses through the cell membrane and is enzymatically hydrolyzed by intracellular esterases to monofluorescent DCFH in the presence of reactive oxygen species [23]. The intensity of fluorescence is proportional to the levels of intracellular reactive oxygen species. Thirty minutes before the end of the treatment time, DCFH-DA (final concentration 5 µM) was added to cell cultures (control or treated with antigorite). Dye-loaded cells were washed with PBS and the fluorescence was monitored in scraped and resuspended cells using a luminescence spectrometer (Perkin-Elmer). The excitation was at $\lambda = 475$ nm and the emission was recorded at $\lambda = 525$ nm.

Determination of Nitrite Release

Nitrite concentration in the supernatant was quantified by colorimetric assay based on the Griess reaction [24] as described by Ding et al. [25]. Briefly, 0.1 ml of the supernatant from untreated or antigorite treated culture was mixed with an equal volume of Griess reagent at room temperature for 10 min. The absorbance was measured at $\lambda = 550$ nm in a microplate spectrophotometer reader (Titertek Multiskan, DAS, Italy). Sodium nitrite was used as a standard.

PGE_2 Determination

The concentration of PGE_2 was measured in the culture media by enzyme-linked immunosorbent assay (ELISA) (Kit Biotrak PGE_2 Amersham Pharmacia Biotech) according to the manufacturer's instructions. Briefly, 50 µl of supernatant was dispensed into 96 wells microplate and 50 µl of diluted antibody and 50µl of diluted conjugate were added. Following incubation at room temperature for 1 h, the cells were washed 4 times with wash buffer and 150 µl of room temperature equilibrate enzyme substrate was added. The plate was mixed on a microtitre plate shaker for 30 min at room temperature. The reaction was stopped by the addition of 100 µl sulphuric acid (1 M) to each well. The optical density of each sample was measured with a microplate spectrophotometer reader (Titertek Multiskan, DAS, Italy) at $\lambda = 450$ nm within 30 min.

Statistical Analysis

Each experiment was repeated at least three times in triplicate and the mean $\pm$ SEM for each value was calculated. Statistical analysis of results was performed using Student's t-test and one-way ANOVA by the statistical software package SYSTAT, version 9 (Systat Inc., Evanston IL, USA). A difference was considered significant at $P < 0.01$.

Results

Antigorite, at concentrations of 5, 50 and 100 µg/ml (1923, 19231, 38461×10^3 fibres, respectively), induced

dose-dependent cytotoxicity in MeT-5A and J774 cells following exposure for 72 hr as revealed by the MTT assay (Figures 5a and 5b).
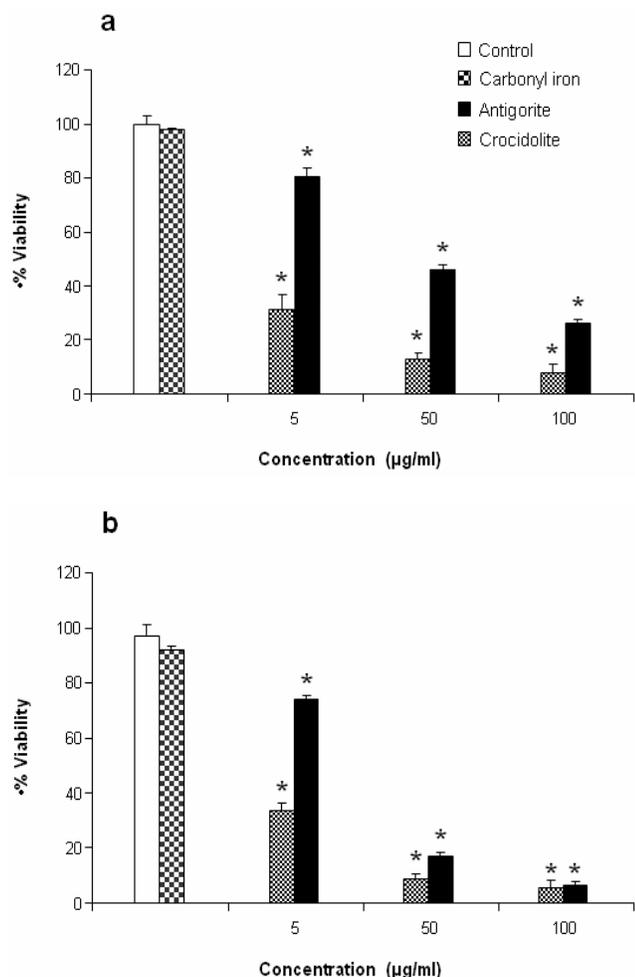

Figure 5: MeT-5A (a) and J774 (b) cell viability measured with tetrazolium salt assay (MTT). The values of optical density measured at $\lambda = 550$ nm are shown as percentage with respect to the optical density registered for untreated control, the latter considered as 100 % of cell viability. The values are the mean ± SEM of three experiments performed in triplicate. All values with P<0.01 were considered significantly different.
* denotes significant difference as compared to untreated control.

This antiproliferative effect was more evident in J774 than in MeT-5A cells, which at 50 and 100 µg/ml of antigorite showed 22 % and 8 % of viability, respectively. In addition, Met-5A and J774 cells showed increasingly higher activity of LDH following exposure to increasing number of antigorite fibers (Figures 6a and 6b). At the end of incubation, LDH leakage in 100 µg/ml antigorite-treated cells was 2.5 and 3.4 times higher than in untreated MeT-5A and J774 cells, respectively.
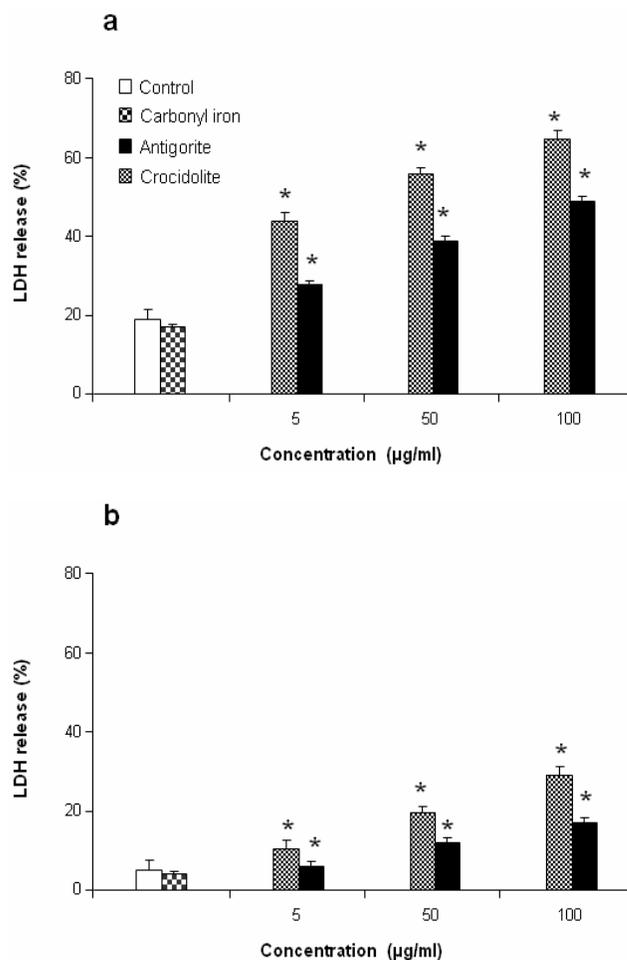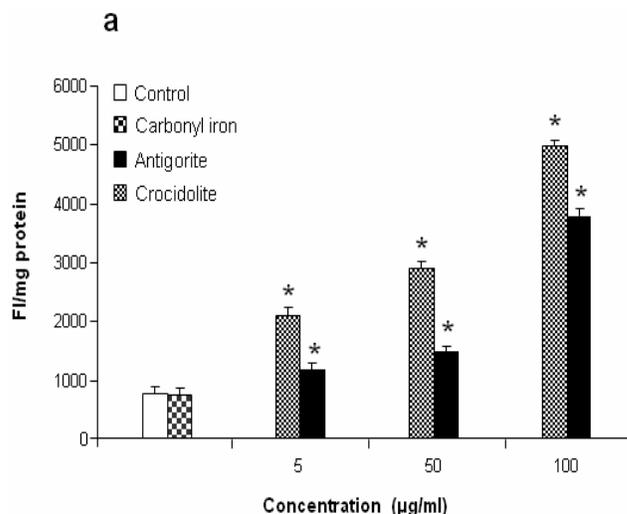

Figure 6: Lactate dehydrogenase (LDH) release from the MeT-5A (a) and J774 (b) cells expressed as percentage of LDH released into the cell medium with respect to total LDH. The values are the mean ± SEM of three experiments performed in triplicate. All values with P <0.01 were considered significantly different from control values and marked with an asterisk.
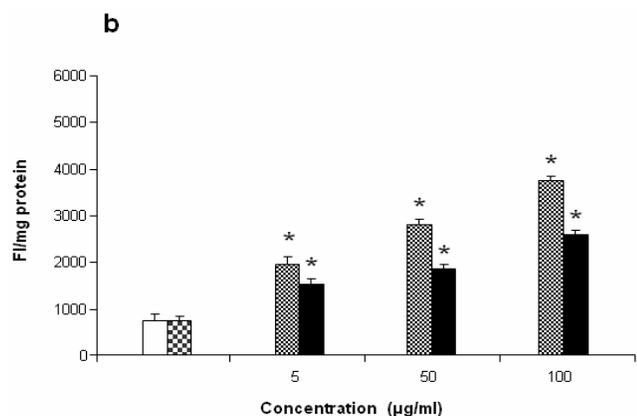
Figure 7: Reactive oxygen species (ROS) production by MeT-5A (a) and J774 (b) cells measured by 2'7'-dichlorodihydrofluorescein diacetate (DCFH-DA) in untreated control and cells treated with various amounts of antigorite. The values, expressed as fluorescence intensity (FI) units per mg of protein, are the mean ± SEM of three experiments performed in triplicate. * - denotes values significantly (P<0.01) different from untreated control.
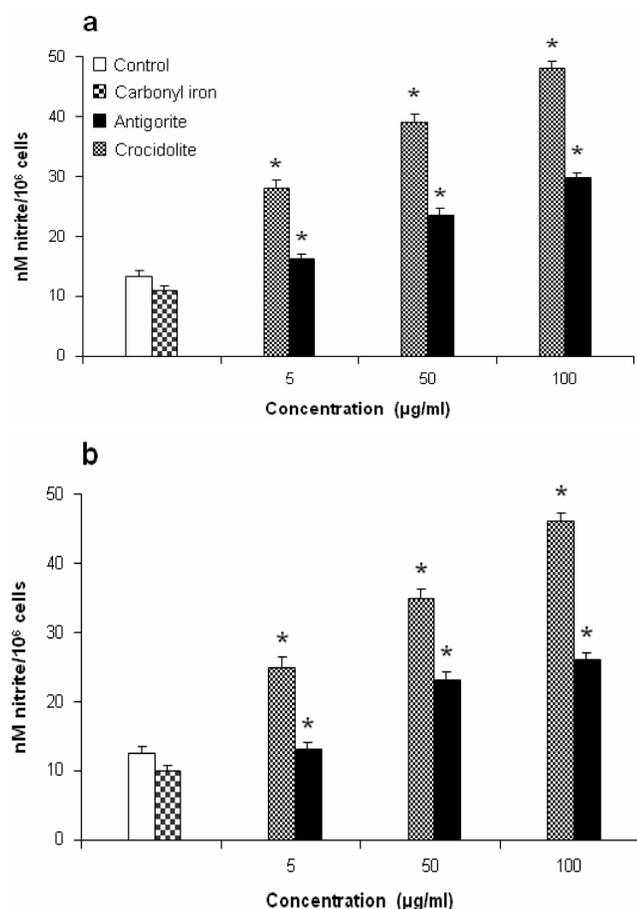

Figure 8: Nitrite release from MeT-5A **(a)** and J774 **(b)** cells quantified by colorimetric assay in the culture media. The values, expressed as nM nitrite per 10^6 cells, are the mean ± SEM of three experiments performed in triplicate. Antigirite caused significant (*, P<0.01) release of nitrite as compared to untreated control experiments.

Figure 7 shows the dose-response relationship of antigorite-induced DCFH-DA fluorescence. Compared to the untreated cells, all three doses of antigorite significantly enhanced the DCFH-DA fluorescence intensity in MeT-5A. In J774 cells, a fluorescence signal was only observed following treatment with 100µg/ml of antigorite. Generation of NO$^\bullet$ was assessed by measuring the concentration of nitrite in the culture medium of Met-5A and J774 cells exposed to fibrous antigorite. As shown in Figure 8a and 8b, in both cell types cultured with antigorite fibres the amount of nitrite was increased.
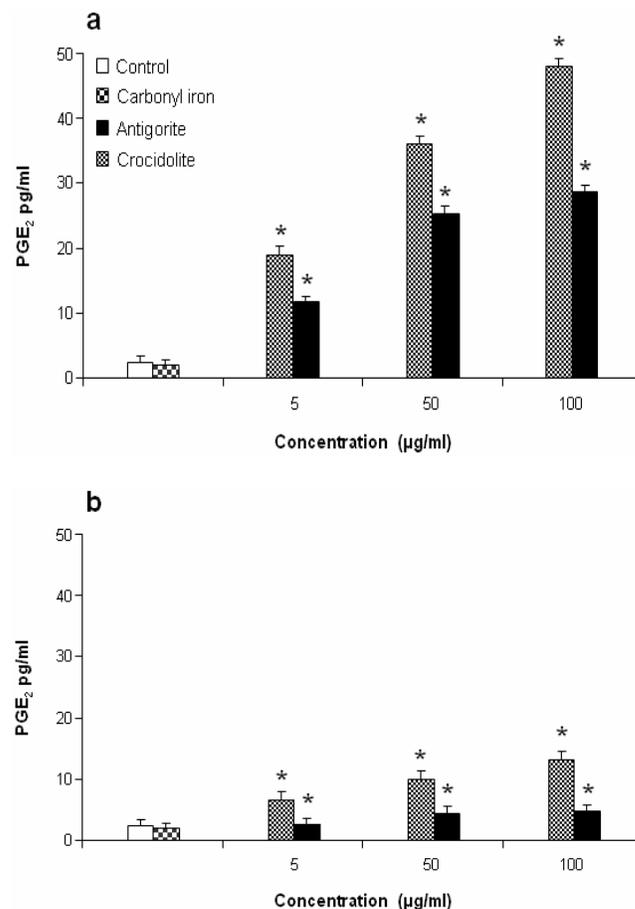

Figure 9: Determination of PGE_2 formation by ELISA in the MeT-5A (a) and J774 (b) cell culture media. The values, expressed as pg/ml, are the mean ± SEM of three experiments performed in triplicate. * - denotes significant differences at P<0.01.

The PGE_2 levels generated by control MeT-5A and J774 cells were 2.4 ± 0.6 pg/ml and 2.4 ± 0.4 pg/ml, respectively (Figure 9a and 9b). Following incubation (72 hrs) with 100 µg/ml of antigorite, the PGE_2 levels were 28.64 ± 1.1 pg/ml and 4.6 ± 1.1 pg/ml in MeT-5A and J774, respectively. Thus, the relative increase in the antigorite-stimulated PGE_2 biosynthesis was 11-fold higher in Met-5A cells compared to about 2-fold increase in J774 cells. Compared to crocidolite, antigorite was a less potent

inhibitor of cell viability and weaker stimulus of COX and LDH activity, and ROS/RNS formation, whereas carbonyl iron spheres were inactive (Figures 5-9).

Discussion

Inhalation of fibrous minerals such as asbestos can cause a variety of respiratory diseases ranging from inflammation and fibrosis to highly malignant forms of cancers [26]. However, questions related to the interaction of fibrous particles with target cells, the molecular mechanisms by which these particles induce cellular damage, and how these events contribute to the pathogenesis of fibroproliferative and malignant diseases as well as the cellular response to the fibrous matter as it relates to carcinogenesis remain unanswered. While some researchers have suggested that asbestos-related disease is a "threshold phenomenon", which requires a certain level of exposure for disease to develop [27], other have argued that there cannot be a safe level of inhaled asbestos [28]. Most common source of contamination is the mechanical damage of materials and surfaces containing asbestos, which stimulates distribution of the airborne asbestos fibers.

About half of the airborne fibre exposures occurring in the Piemonte (Italy) area are asbestiform fibers that are not commonly included in exposure assessments under the current asbestos analytical protocols and regulatory definitions. Most current regulations and approved analytical methods for asbestos exclude other fibrous and asbestiform minerals. In the early 2000, it became apparent that asbestos-like fibres in the Penninic Piemonte Zone of the Western Alps were responsible for significant illness in the local population [5-7]. Recent studies have shown that, in addition to chrysotile, tremolite, balangeroite and carlosturanite, the minerals antigorite, diopside, olivine, brugnatellite and brucite having asbestiform properties are present in the Piemonte Zone of the Western Alps [5-7]. Differences in chemistry and morphology create health problems, including difficulties in identification and complications in relating exposures to existing toxicological studies. Mineralogical characterization of rocks mined from specific deposits has helped to characterize the presence, form, abundance, and morphology of potential asbestos-like toxicants. *In vitro* toxicity tests of well-characterized ore can help the understanding of toxicity effects of potential toxicants upon exposure present in rocks, soils, dusts, and water as a result of natural erosion and weathering of mineral deposits and host rocks.

The three minerals, chrysotile, antigorite and lizardite, have a very similar chemical composition, but significantly different structures [5-7]. In fact, a single general chemical formula $(OH)_3Mg_3[Si_2O_5(OH)]$ corresponds to several crystal structures that represent different solutions for the minimization of the mismatch between sheets of SiO_4 tetrahedra and sheets of $MgO_2(OH)_4$ octahedra. Biological effects of many of these minerals have not been characterized and our study is the first to characterize the responses of cells to antigorite fibers. Our study investigated the cellular toxicity and some biochemical parameters in mesothelial MeT-5A and monocyte-macrophage J774 cell lines, widely employed in studies on the lung disease models. The aim of this investigation was to gain suggestions on the potentiality of fibrous antigorite to be harmful to humans.

Fibrous antigorite induces a dose-dependent decrease of cell viability of both MeT-5A and J774, suggesting that it interferes with the proliferation of target cells, particularly of the J774. This decrease is associated with an increase of LDH release in cell medium, representing a breakdown of cell membrane, hallmark of cell death and widely used to measure the cytotoxicity both *in vivo* and *in vitro* [29]. Our results indicate a potent cytotoxic effect of antigorite at 100 µg/ml, as in both cells the percentage of LDH leakage was about two times higher than the controls. The initial interaction between silica particles and cell membrane is believed to be through hydrogen bonding, or free-radical-mediated reaction, or both [30].

ROS have been recognized as important early intermediates of cell injury and death in various pathophysiologic processes and implicated in pulmonary diseases caused by several environmental pollutants [29]. We found that in the MeT-5A cells, antigorite elevated the ROS and $NO^\bullet$ production in a dose-dependent manner. The J774 cells generated significant levels of $NO^\bullet$ and ROS only following exposure to the high dose of antigorite. These results confirm that mesothelial cells and macrophages exposed to antigorite generated ROS and $NO^\bullet$. This observation suggests the possibility that mesothelial cells may be a source of ROS and $NO^\bullet$-derived radicals such as the nitrogen dioxide (NO_2) and may undergo oxidative stress when exposed to fibrous antigorite. Both ROS and RNS induce inflammatory reactions and/or cell transformation in adjacent tissues [31, 32]. On a molecular level, exposure to ROS and RNS induces modifications of critical cellular components such as lipids via mechanisms of lipid peroxidation and nitration [16]. We noticed that the J774 cells were less sensitive to antigorite than the MeT-5A cells. Similar trend was observed with PGE_2 generation in these two cell lines. Products of arachidonic acid metabolism are critical participants in the development of inflammatory responses after infection or tissue injury. PGE_2, derived from the COX enzyme, is one of the most studied mediators of this process. Mammalian cells contain two related isoforms of COX referred to as COX-1 and COX-2. The latter is expressed after exposure to mitogenic or pathological stimuli. Ding et al. have reported that nuclear factor kappa B (NF-□□) plays a key regulatory role in the expression of genes related to several inflammatory mediators and may be important in silica-induced COX-2 gene transcription [15]. We have shown that a minor increase of ROS production in J774 macrophages leads to a minor expression of PGE_2 induced by antigorite. Numerous investigations have established the importance of PGE_2 formed by COX-2 catalysis in the modulation cellular processes that govern cell growth and differentiation, by

inducing the antiapoptotic Bcl-2 protooncogene, enhancing angiogenesis and adhesion by modulating integrin expression, and elevating intracellular cyclic AMP, which suppresses apoptosis [14, 15].

The pathogenesis of asbestos-associated diseases is related with a persistent inflammatory response initiated directly or indirectly by ROS, cytokines, chemokines, growth factors, and pro-inflammatory factors. These secretions trigger activation of transcription factors and mitogen-activated protein kinases (MAPK), which are linked to early response genes. Pro-inflammatory gene responses appear to be regulated at the transcriptional level by DNA binding proteins that are under the influence of ROS [33,34]. Our results show a more pronouced pro-inflammatory effect of antigorite on mesothelial cells than on the macrophages cells. These results indicate that not all iron-containing minerals had the same level of activity on different types of cells. Iron present in the bulk of iron-containing minerals is important in reducing O_2 via participation in a Fenton-type reaction. Studies have shown that the ability of asbestos fibres to elicit these effects is not related to total iron content, suggesting the presence of specific iron active sites that exist at the surface and become active in free radical generation only when present at specific crystallographic sites in a definite valency and coordination state [1]. In addition to ROS-induced effects, toxicity by asbestos may be modulated by $NO^\bullet$-derived oxidants, peroxynitrite ($ONOO^-$) and nitrogen dioxide (NO_2). Increased levels of nitrites/nitrates by alveolar macrophages and mesothelial cells has been demonstrated after exposure to different types of asbestos fibres [35,36]. Thus, although crocidolite, the most carcinogenic type of asbestos, induced higher effects, antigorite-induced upregulation of $NO^\bullet$ in the lungs from macrophages, as well as the induction of inflammation from mesothelial cells, may contribute to the pathogenesis of lung injury. The results of this study revealed significant biochemical changes in mesothelial MeT-5A and monocyte-macrophage J774 cells after fibrous antigorite treatment and suggested that these changes may directly or indirectly be the one of the biological events responsible for eliciting of antigorite-mediated host pathological or neoplastic responses.

References

1. Kamp, D. W.; Weitzman, S. A.: The molecular basis of asbestos induced lung injury. *Thorax*, **1999,** *54,* 638-652.
2. Gavett, S. H. Physical characteristics and health effects of aerosols from collapsed buildings. *J. Aerosol Med.* **2006,** *19,* 84-91.
3. Shukla, A.; Gulumian, M.; Hei, T. K.; Kamp, D.; Rahman, Q.; Mossman, B. T.: Multiple roles of oxidants in the pathogenesis of asbestos-induced diseases. *Free Radic. Biol. Med.,* **2003,** *34,* 1117-1129.
4. Rohl, A. N.; Langer, A. M.; Selikoff, I. J. Environmental asbestos pollution related to use of quarried serpentine rock. *Science,* **1977,** *196,* 1319-1322.
5. Belluso, E.; Compagnoni, R.; Ferraris, G. Occurrence of asbestiform minerals in the serpentinites of the Piemonte Zone, Western Alps. *Giornata di Studio in Ricordo del Prof. Stefano Zucchetti, Politechnico di Torino,* **1995,** 57-64.
6. Groppo, C.; Rinaudo, C.; Gastaldi, D. Micro-Raman spectroscopy for a quick and reliable identification of serpentine minerals from ultramafics. *Eur. J. Miner.* **2007,** *in press.*
7. Rinaudo, C.; Gastaldi, D.; Belluso, E. Characterization of chrysotile, antigorite and lizardite by FT Raman spectroscopy. *Can. Miner.,* **2003,** *41,* 883-890.
8. Groppo, C.; Tomatis, M.; Turci, F.; Gazzano, E.; Ghigo, D.; Compagnoni, R.; Fubini, B.: Potential toxicity of nonregulated asbestiform minerals: balangeroite from the western Alps. Part 1: Identification and characterization. *J. Toxicol. Environ. Health A,* **2005,** *68,* 1-19.
9. Harf, R.; Laval, I.; Davezies, P.; Prost, G. [Unrecognized occupational risk of pleural mesothelioma. The example of the Rhone-Alps region, *Rev. Mal. Respir.,* **1993**, *10,* 453-458.
10. Fubini, B.; Otero Arean, C.: Chemical aspects of toxicity of inhaled mineral dusts. *Chem. Soc. Rev.* **1999,** *28,* 373-381.
11. Shukla, A.; Ramos-Nino, M.; Mossman, B.: Cell signaling and transcription factor activation by asbestos in lung injury and disease. *Int. J. Biochem. Cell Biol,.* **2003,** *35,* 1198-1209.
12. Pelin, K.; Hirvonen, A.; Taavitsainen, M.; Linnainmaa, K. Cytogenetic response to asbestos fibers in cultured human primary mesothelial cells from 10 different donors. *Mutat. Res.,* **1995,** *334,* 225-233.
13. Fenoglio, I.; Croce, A.; Di Renzo, F.; Tiozzo, R.; Fubini, B. Pure-silica zeolites (Porosils) as model solids for the evaluation of the physicochemical features determining silica toxicity to macrophages. *Chem Res. Toxicol.,* **2000,** *13,* 489-500.
14. Fitzpatrick, F. A. Inflammation, carcinogenesis and cancer. *Int. Immunopharmacol.,* **2001,** *1,* 1651-1667.
15. Ding, M.; Chen, F.; Shi, X.; Yucesoy, B.; Mossman, B.; Vallyathan, V. Diseases caused by silica: mechanisms of injury and disease development. *Int. Immunopharmacol.,* **2002,** *2,* 173-182.
16. Balazy, M.; Poff, C. D.: Biological nitration of arachidonic acid. *Curr. Vasc. Pharmacol.* **2004,** *2,* 81-93.
17. DeWitt, D. L. Prostaglandin endoperoxide synthase: regulation of enzyme expression. *Biochim. Biophys. Acta* , **1991,** *1083,* 121-134.
18. Capitani, G.; Mellini, M. HRTEM evidence for 8-reversals in the m = 17 antigorite polysome. *Am. Miner.,* **2005,** *90,* 991-999.
19. Capitani, G.; Mellini, M. The modulated crystal structure of antigorite: the m = 17 polysome. *Am. Miner.,* **2004**, *89,* 147-158.

20. Mosmann, T. Rapid colorimetric assay for cellular growth and survival: application to proliferation and cytotoxicity assays. *J. Immunol. Methods,* **1983**, *65,* 55-63.

21. Bradford, M. M.: A rapid and sensitive method for the quantitation of microgram quantities of protein utilizing the principle of protein-dye binding. *Anal. Biochem.,* **1976**, *72,* 248-254.

22. Renis, M.; Cardile, V.; Russo, A.; Campisi, A.; Collova, F.: Glutamine synthetase activity and HSP70 levels in cultured rat astrocytes: effect of 1-octadecyl-2-methyl-rac-glycero-3-phosphocholine. *Brain Res.,* **1998,** *783,* 143-150.

23. Shen, H. M.; Shi, C. Y.; Shen, Y.; Ong, C. N. Detection of elevated reactive oxygen species level in cultured rat hepatocytes treated with aflatoxin B1. *Free Radic. Biol. Med.,* **1996,** *21,* 139-146.

24. Green, L. C.; Wagner, D. A.; Glogowski, J.; Skipper, P. L.; Wishnok, J. S.; Tannenbaum, S. R.: Analysis of nitrate, nitrite, and [15N]nitrate in biological fluids. *Anal. Biochem.,* **1982,** *126,* 131-138.

25. Ding, A. H.; Nathan, C. F.; Stuehr, D. J.: Release of reactive nitrogen intermediates and reactive oxygen intermediates from mouse peritoneal macrophages. Comparison of activating cytokines and evidence for independent production. *J. Immunol.,* **1988**, *141,* 2407-2412.

26. Hessel, P. A.; Gamble, J. F.; McDonald, J. C.: Asbestos, asbestosis, and lung cancer: a critical assessment of the epidemiological evidence. *Thorax* **2005,** *60,* 433-436.

27. Ilgren, E. B.; Browne, K.: Asbestos-related mesothelioma: evidence for a threshold in animals and humans. *Regul. Toxicol. Pharmacol.* **1991**, *13,* 116-132.

28. Egilman, D. S.; Reinert, A. A.: The origin and development of the asbestos Threshold Limit Value: scientific indifference and corporate influence. *Int. J. Health Serv.,* **1995,** *25,* 667-696.

29. Jackson, A. L.; Loeb, L. A.: The contribution of endogenous sources of DNA damage to the multiple mutations in cancer. *Mutat. Res.* **2001**, *477,* 7-21.

30. Zhang, Z.; Shen, H. M.; Zhang, Q. F.; Ong, C. N.: Involvement of oxidative stress in crystalline silica-induced cytotoxicity and genotoxicity in rat alveolar macrophages. *Environ. Res.,* **2000,** *82,* 245-252.

31. Erdogdu, G.; Hasirci, V.: An overview of the role of mineral solubility in silicosis and asbestosis. *Environ. Res.,* **1998**, *78,* 38-42.

32. Rahman, I.; Gilmour, P. S.; Jimenez, L. A.; MacNee, W.: Oxidative stress and TNF-a induce histone acetylation and NF-κB/AP-1 activation in alveolar epithelial cells: potential mechanism in gene transcription in lung inflammation. *Mol. Cell Biochem.,* **2002**, *234-235,* 239-248.

33. Rola-Pleszczynski, M.; Gouin, S.; Begin, R. Asbestos-induced lung inflammation. Role of local macrophage-derived chemotactic factors in accumulation of neutrophils in the lungs. *Inflammation,* **1984**, *8,* 53-62.

34. Manning, C. B.; Vallyathan, V.; Mossman, B. T. Diseases caused by asbestos: mechanisms of injury and disease development. *Int. Immunopharmacol.*, **2002**, *2,* 191-200.

35. Quinlan, T. R.; BeruBe, K. A.; Hacker, M. P.; Taatjes, D. J.; Timblin, C. R.; Goldberg, J.; Kimberley, P.; O'Shaughnessy, P.; Hemenway, D.; Torino, J.; Jimenez, L. A.; Mossman, B. T.: Mechanisms of asbestos-induced nitric oxide production by rat alveolar macrophages in inhalation and in vitro models. *Free Radic. Biol. Med.,* **1998**, *24,* 778-788.

36. Choe, N.; Tanaka, S.; Kagan, E. Asbestos fibers and interleukin-1 upregulate the formation of reactive nitrogen species in rat pleural mesothelial cells. *Am. J. Respir. Cell Mol. Biol.,* **1998**, *19,* 226-236.